optica

Quantum-enhanced interferometry with weak thermal light

Seyed Mohammad Hashemi Rafsanjani,[1,*] Mohammad Mirhosseini,[1] Omar S. Magaña-Loaiza,[1] Bryan T. Gard,[2] Richard Birrittella,[3] B. E. Koltenbah,[4] C. G. Parazzoli,[4] Barbara A. Capron,[4] Christopher C. Gerry,[3] Jonathan P. Dowling,[2] and Robert W. Boyd[1,5]

[1]Institute of Optics, University of Rochester, Rochester, New York 14627, USA
[2]Hearne Institute for Theoretical Physics and Department of Physics and Astronomy, Louisiana State University, Baton Rouge, Louisiana 70803, USA
[3]Department of Physics and Astronomy, Lehman College, The City University of New York, Bronx, New York 10468, USA
[4]Boeing Research & Technology, Seattle, Washington 98124, USA
[5]Department of Physics, University of Ottawa, Ottawa, Ontario K1N6N5, Canada
*Corresponding author: shashem2@ur.rochester.edu

Received 22 August 2016; revised 16 February 2017; accepted 27 March 2017 (Doc. ID 274217); published 20 April 2017

We propose and implement a procedure for enhancing the sensitivity with which one can determine the phase shift experienced by a thermal light beam possessing on average fewer than four photons in passing through an interferometer. Our procedure entails subtracting exactly one (which can be generalized to m) photon from the light field exiting an interferometer containing a phase-shifting element in one of its arms. As a consequence of the process of photon subtraction, the mean photon number and signal-to-noise ratio (SNR) of the resulting light field are increased, leading to an enhancement of the SNR of the interferometric signal for that fraction of the incoming data that leads to photon subtraction.

OCIS codes: (270.0270) Quantum optics; (270.5290) Photon statistics; (120.3180) Interferometry; (120.3940) Metrology.

https://doi.org/10.1364/OPTICA.4.000487

1. INTRODUCTION

Interferometry is the technique of choice for many of the most sensitive physical measurements to date [1]. It underlies many monumental discoveries in physics, such as Young's double-slit experiment, the Michelson–Morley experiment that established the special theory of relativity, and recently and spectacularly in gravitational wave detection [1]. Many such applications deal with sources of light that possess thermal statistics. The fluctuations in the number of photons of a thermal state are given by $\sqrt{\bar{n}(\bar{n}+1)}$, where $\bar{n}$ is the average number of photons contained in the field. For a dim source of thermal light, the magnitude of these fluctuations becomes comparable to or even larger than $\bar{n}$.

The most straightforward approach for increasing the signal-to-noise ratio (SNR) of an interferometric signal is to increase the signal. For a fixed source of illumination, however, this approach can be realized only at the expense of increasing the measurement time. In this communication, we seek alternative methods of enhancing the SNR for a given value of average photon number. We seek to develop a tool to distill the interferometric data even for quantum states that include only a few photons. Naively, one may expect that amplifying the input to an interferometer may lead to enhanced interferometry. However, quantum mechanics dictates a minimum noise cost that erases any benefit that amplification provides [2]. We thus need to go beyond unitary operations to improve the sensitivity of an interferometric setup for an input beam containing only a few thermal photons. Furthermore, although there are multiple strategies developed to harness the quantum nature of light in order to enhance the accuracy of interferometric measurements [3–8], such proposals use exotic quantum states of light, e.g., squeezed states or entangled states, to probe the physical process of interest [3,9–15]. Unfortunately such an arrangement is infeasible when the object of interest is a remote source of light that possesses thermal statistics. We thus instead make use of a postprocessing operation to distill the statistical information already contained in the interferometric signal [16–19].

Here we describe a means of enhancing the phase sensitivity of dim-light interferometry. Our method is based on the use of photon-subtracted thermal states, which are states obtained by removing a fixed number of photons from a light field that possesses thermal statistics [20,21]. Photon-subtracted states have recently attracted interest because of their applications in quantum communication, quantum computation, and quantum metrology [20,22–31]. In contrast with the conventional approach of utilizing quantum states as the input to the interferometer, we propose to implement photon subtraction on the light exiting the interferometer. Surprisingly, such a subtraction scheme leads to an enhancement in both the magnitude of the signal and the SNR, and we demonstrate this in a scenario where the average number of photons in the interferometer is fewer than four photons.

2. PHOTON-SUBTRACTED ENHANCEMENT OF INTERFEROMETRY

We first propose a simple model to capture the essence of how photon subtraction enhances both the signal strength and the SNR in interferometry. An interferometer is mathematically equivalent to a phase-dependent unitary transformation that connects the input ports $(\hat{a}, \hat{b})$ to those of the output ports $(\hat{c}, \hat{d})$. For simplicity we assume the interferometer to be symmetric; that is, the beam splitters are 50% transmitting and 50% reflecting. The field operators of the output ports are then related to those of the input ports through the following transformation:

$$\hat{c} = \frac{1}{2}[(e^{i\varphi} - 1)\hat{b} + i(e^{i\varphi} + 1)\hat{a}],$$
$$\hat{d} = \frac{1}{2}[i(e^{i\varphi} + 1)\hat{b} + (1 - e^{i\varphi})\hat{a}], \quad (1)$$

where φ denotes the phase difference between the two paths.

We assume that input port $\hat{a}$ is fed by thermal light and that port $\hat{b}$ is fed by the vacuum state. In this case the fields at both output ports possess thermal statistics whose averages and standard deviations are [32]

$$\bar{n}_c = \mathrm{Tr}[\hat{c}^\dagger \hat{c}\hat{\rho}_0] = \bar{n}\cos^2\frac{\varphi}{2}, \qquad \Delta n_c = \sqrt{\bar{n}_c^2 + \bar{n}_c},$$
$$\bar{n}_d = \mathrm{Tr}[\hat{d}^\dagger \hat{d}\hat{\rho}_0] = \bar{n}\sin^2\frac{\varphi}{2}, \qquad \Delta n_d = \sqrt{\bar{n}_d^2 + \bar{n}_d}. \quad (2)$$

Here $\bar{n} = \mathrm{Tr}[\hat{a}^\dagger \hat{a}\hat{\rho}_{\mathrm{th}}]$ is the average occupation number in input port $\hat{a}$. Note that although the initial density matrix describes a separable state of the form $\hat{\rho}_0 = \hat{\rho}_{\mathrm{th}}^{(a)} \otimes \hat{\rho}_{\mathrm{vac}}^{(b)}$, the output is not a direct product of the two reduced density matrices of the output ports. However, the reduced density matrix for either of the output ports is itself that of a thermal state [32].

Our strategy for enhancing the measurement sensitivity is to suppress the zero photon events of the thermal light distribution. Note that the most probable photon occupation number in a thermal state is the vacuum state. However, the vacuum does not produce any detection event. Therefore by suppressing the vacuum contribution of the thermal distribution we achieve an ensemble that has a higher probability of producing a signal at detectors. Our means for suppressing the vacuum contribution is photon subtraction, which can increase the average number of photons in the resulting light field [20,33]. After implementing the subtraction, the resulting reduced density matrix for port $\hat{c}$ is (see Supplement 1)

$$\hat{\rho}_{1c} = \sum_n \frac{(n+1)\bar{n}_c^n}{(1+\bar{n}_c)^{n+2}} |n\rangle_c\,{}_c\langle n|. \quad (3)$$

Here $|n\rangle_c$ is the Fock state of n photons in port $\hat{c}$. For this photon-subtracted state the average photon number and its variance are

$$\mathrm{Tr}[\hat{c}^\dagger \hat{c}\hat{\rho}_{1c}] = 2\bar{n}\cos^2\frac{\varphi}{2} = 2\bar{n}_c,$$
$$(\mathrm{Tr}[(\hat{c}^\dagger \hat{c})^2\hat{\rho}_{1c}] - \mathrm{Tr}[\hat{c}^\dagger \hat{c}\hat{\rho}_{1c}]^2)^{1/2} = \sqrt{2}\Delta n_c. \quad (4)$$

Thus subtraction of a single photon from port $\hat{c}$ doubles the average number of photons and the variance. The SNR, defined as the ratio of the mean photon number to its standard deviation, is then enhanced by a factor of $\sqrt{2}$. Interestingly, the same enhancement occurs for photons in port $\hat{d}$ after conditioning on subtraction of a single photon from port $\hat{c}$. Furthermore, removing a larger number of photons from the input thermal state leads to an even more pronounced increase in the mean and SNR.

In the discussion just presented, we did not account for the effects of various loss mechanisms. However, we have shown elsewhere that even when such losses are included, the enhancement due to photon subtraction remains considerable [34]. From the full model the average and standard deviation of the number of detection events associated with port c are given by

$$\bar{N}_c = \bar{n}T\eta_2\cos^2\frac{\varphi}{2}\left(\delta_{0m} + \frac{(1-\delta_{0m})(m+1)}{1+\bar{n}(1-T)\eta_1\cos^2\frac{\varphi}{2}}\right),$$
$$\Delta N_c = \bar{N}_c \Big/ \sqrt{\frac{(1+m)\bar{n}T\eta_2\cos^2\frac{\varphi}{2}}{1+\bar{n}(T\eta_2 + (1-T)\eta_1)\cos^2\frac{\varphi}{2}}} \quad (5)$$

Here η_i is the detection efficiency at detector i, T denotes the transmission of the beam splitter used for subtraction, m is the number of subtracted photons, and δ_{0m} is the Kronecker delta function.

3. EXPERIMENTAL REALIZATION

Next we describe the experiment we used to demonstrate the enhancement in measurement sensitivity. Our demonstration provides, to the best of our knowledge, the first direct observation of the enhancement in SNR that is achieved by implementing the process of photon subtraction. A schematic representation of our setup is shown in Fig. 1. We use a narrow-band external-cavity diode laser operating at a wavelength of 780 nm. To produce thermal statistics we focus the cw beam from the laser onto a rotating ground-glass plate. The beam is then coupled into a single-mode optical fiber to extract a single transverse mode of pseudothermal light [35]. We next pass this beam through the interferometer. In our implementation we use a common-path Mach–Zehnder interferometer (MZI). In such an implementation the two polarizations of light correspond to the different arms of the interferometer. The phase difference between the two polarizations is

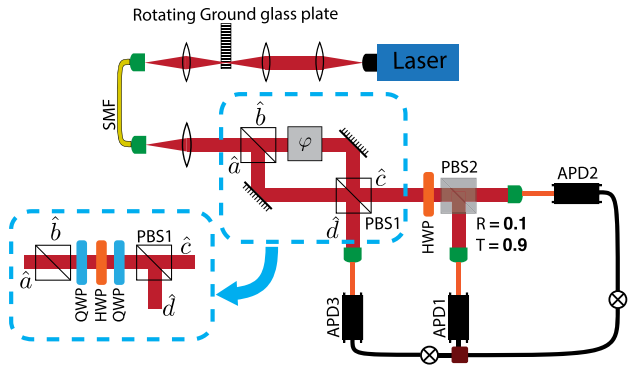

Fig. 1. Schematic of the experimental setup used to observe increased measurement sensitivity through photon subtraction. The output beam from a narrow-bandwidth cw laser is focused onto a rotating ground-glass plate and is then coupled into a single-mode optical fiber (SMF). The single-transverse-mode, thermal light exiting the SMF is then sent to one input port ($\hat{a}$) of a Mach–Zehnder interferometer (MZI). Light from one output port ($\hat{c}$) is then sent to a combination of a half-wave plate (HWP) and polarizing beam splitter (PBS2) to perform the process of photon subtraction. Detector APD2 counts the number of photons in a time window of fixed length, conditioned on a detection event in APD1. Similarly, light from the other output port ($\hat{d}$) is sent to detector APD3. In our actual implementation (see inset), we use a common-path MZI to increase the stability. In this case a rotatable HWP is used to control the phase difference between two orthogonal polarization states of the light beam.

set by means of a rotatable half-wave plate (HWP) placed within the interferometer. The phase difference determines the relative intensities of the light at the two output ports. It is our goal to determine this phase difference with high accuracy.

Without photon subtraction, our measurement sensitivity is limited by the standard fluctuations from each of the output ports of the interferometer. We increase the sensitivity through the process of photon subtraction, which we implement as follows. We divert as little as (10%) of one of the output ports to detector APD1. The fraction of the light sent to this detector is controlled by a HWP and a polarizing beam splitter (PBS2). The number of "clicks" within one integration time of $\simeq 1$ μs indicates the number of photons subtracted from the field. We then count the number of detection events for detectors APD2 and APD3 conditioned on the number of detection events measured by APD1. Note that our subtraction scheme works on a random basis and will be successful only about 10% of the time. Nevertheless, we note that there are other schemes for photon subtraction that lead to a higher success rate in postselection [27,36,37].

We first establish a baseline experiment with which the photon-subtracted results can be compared. We set the phase difference such that port $\hat{d}$ becomes dark and all the photons are directed toward port $\hat{c}$. We then change the induced phase by rotating the HWP inside the MZI. For each value of the phase we register the number of photons that are detected in each coherence time. From this data we extract a histogram of the number of detected photons, which we then normalize to produce a probability distribution [Fig. 2(a)]. We also extract the average [Fig. 2(b)] and the SNR [Fig. 2(c)] of the histogram for each value of the phase. For all values of the phase, we observe negative exponential distributions (the signature of a thermal source) whose average occupation numbers are $\bar{n}T\eta_2 \sim 1.1\cos^2(\varphi/2)$. Note that the value of $\bar{n}$ is determined through the average number of detected photons after taking account of the various efficiencies (losses) of the detection process.

We next demonstrate the effect of photon subtraction on the sensitivity of the interferometer by plotting the same quantities when subtraction is implemented. We perform photon counting through the use of avalanche photodiodes (APDs) operating in the Geiger mode. The coherence time of our laser is approximately 1 μs, and to ensure that we perform measurements on a single-temporal-mode field, we use an integration time equal to the coherence time. The deadtime of our APD detectors is approximately 50 ns. To minimize errors associated with the arrival of a second photon within the deadtime following a specific detection event, we adjust our laser intensity so that only a small number ($\lesssim 4$) of photons arrive in any one integration time. We also use a statistical approach to correct our raw data for the rare occurrence of multiple photons arriving within detector deadtime; see Supplement 1 for details. Our use of a long-coherence-time light source allows us to time-bin the output of a standard APD to perform photon counting, thus circumventing the need to use photon-number-resolving detectors [21].

In Fig. 3(a), we show a histogram of the photon number distribution measured at APD2 conditioned on the detection of a photon in the APD1 for different values of φ. In Figs. 3(b) and 3(c), we plot the mean photon number and the SNR as functions of φ. For comparison, we have also included the results for light with pure thermal statistics. We see that photon subtraction leads to an increase of the average photon number and SNR. For $\varphi = 0$ the mean is increased from 1.1 to 1.8 and the SNR is increased from 0.86 to 1.15. The results are in very good agreement with the predictions of Eq. (7). Note that the increase in mean number is less than a factor of 2 and the increase in SNR is less than a factor of $\sqrt{2}$ as a consequence of loss. Nevertheless, even in the presence of loss we observe considerable enhancement in both signal and SNR.

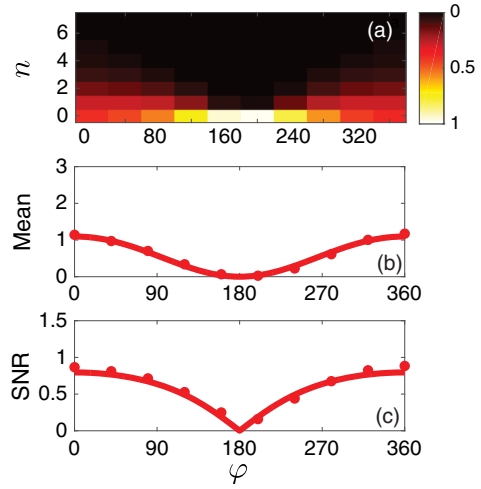

Fig. 2. (a) Probability distribution of the photon number distribution. Each column corresponds to a given value of the phase, and the probability is encoded in the color coding. (b) Mean photon number and (c) signal-to-noise ratio measured at the output of the interferometer by APD2 as a function of the phase difference between the two arms of the interferometer. Each column in panel (a) corresponds to a dot in panels (b) and (c). Dots represent experimental results, and the solid lines describe what is expected from theory. Here the average photon number before the interferometer is $\bar{n} = 4.1$, the transmission of the subtracting PBS is $T = 0.9$, the detection efficiency of APD2 is $\eta_2 \approx 0.3$, and $\bar{N}_c = 1.1$.

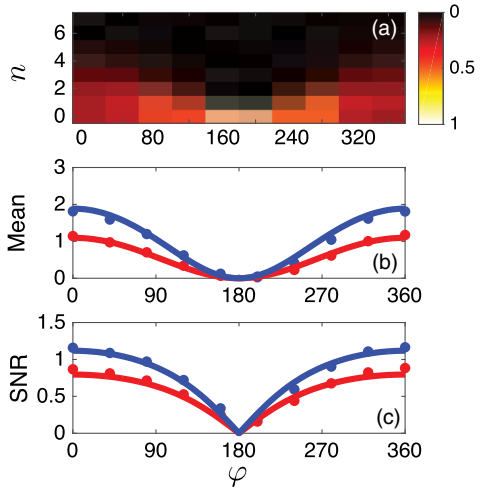

Fig. 3. (a) Probability distribution of the photon number distribution. Each column corresponds to a given value of the phase, and the probability is encoded in the color coding. (b) Mean photon number (blue) and (c) signal-to-noise ratio (blue) measured at the output of the interferometer by APD2 as a function of the phase difference between the two arms of the interferometer. Each column in panel (a) corresponds to a dot in panels (b) and (c). Dots represent experimental results, and the solid lines describe what is expected from theory. The parameters are the same as in Fig. 2, and the detection efficiency of APD1 is $\eta_1 \approx 0.33$. Also in red are the results for thermal light without subtraction for comparison.

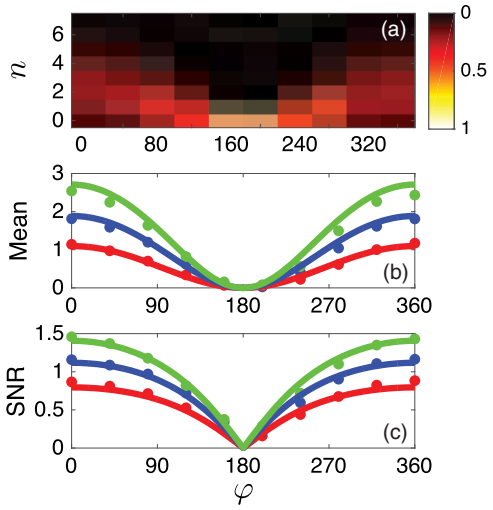

Fig. 4. Same as Fig. 3, except for two-photon-subtracted thermal light. Also shown are the results for thermal light without subtraction (in red) and one-photon-subtracted thermal light (in blue) for comparison.

Subtracting more than one photon leads to an even more pronounced increase in the mean photon number and SNR, as in Eq. (7). We show results for the case of two-photon-subtracted thermal states in Fig. 4. We obtain these results by conditioning the photon registration by APD2 on the detection of two photons by APD1. We observe a pronounced departure from the negative exponential distribution. For $\varphi = 0$ the mean occupation number increases from 1.14 without conditioning to 2.54, and the SNR increases from 0.86 to 1.45. In Figs. 4(b) and 4(c) we plot the mean and SNR as functions of φ. Besides the excellent agreement between the theory and experiment, these results confirm the increase in enhancement due to two-photon subtraction. We note that subtraction of a larger number of photons should lead to a further increase in both average occupation number and SNR.

The above results demonstrate the increase in the mean photon number and SNR of the light from output port c conditioned on the subtraction photons from the same output port. Theory interestingly predicts that photon subtraction from port c also enhances the mean photon number and SNR for light leaving from port d. In Fig. 5 we plot the data to demonstrate this effect.

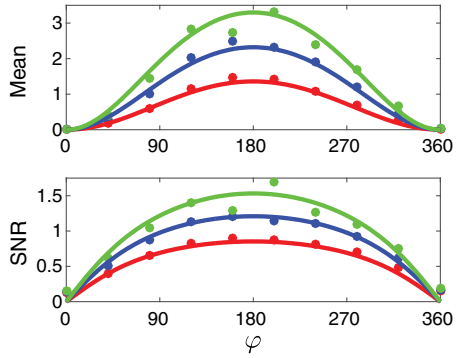

Fig. 5. Average occupation number (top) and signal-to-noise ratio (bottom) at the other output port $\hat{d}$ of the MZI measured as a function of the phase shift introduced within the interferometer. The dots represent the experimental results, and the lines are the theoretical predictions. Here $\bar{n} = 4.1$, $T = 0.9$, $\eta_3 \sim 0.42$, and $\eta_1 \sim 0.33$. Also included are the nonconditioned and one-photon-subtracted thermal light for comparison.

We see that the mean photon number and SNR of port d are increased by the process of photon subtraction from port c, and that the increase becomes more pronounced for the subtraction of two photons. This surprising dependence of the photon number distribution involving the two ports is a manifestation of the correlations between the output ports c, d in the joint density matrix.

We emphasize the connection between photon subtraction and photon bunching. The fact that subtracting a photon leads to an enhancement in the signal and SNR is connected to the fact that in a thermal distribution the photons are *bunched*. Thus a subtraction event signals the higher probability for the presence of photons in the signal detector.

4. POSTSELECTION LOSS ANALYSIS

Our results show that the SNR of the interferometric signal can be enhanced by using photon subtraction. However, our specific realization of this idea is based on a non-deterministic physical process (i.e., reflection from a weak beam splitter). Due to this, our procedure accompanies a postselection loss of some of the events, and this loss hampers the sensitivity of the interferometer. Below we study this loss and its effect on the overall sensitivity.

The phase sensitivity of an interferometer can be characterized by

$$\delta\phi = \Delta s \left(\frac{\partial s}{\partial \phi}\right)^{-1}, \tag{6}$$

where s is the signal and Δs is the standard deviation of this quantity. If we gather data from m "clicks," our total signal is $s = m\bar{N}$, where $\bar{N}$ is the average number of detected photons at APD2. If we compare two different schemes of interferometry with the same number of measurements (m), one can ignore the number of measurements. We can also use expressions (2)–(4). For unconditioned measurements we use $\bar{N} = n_c$ and $\Delta N = \Delta n_c$, and for the subtracted scheme we use $\Delta N_{\text{sub}} = \sqrt{2}\Delta n_c$ and $\bar{N}_{\text{sub}} = 2\bar{n}_c$. The sensitivity of the subtracted scheme and the unconditioned scheme can be compared as the following:

$$\delta\phi_{\text{sub}} = \Delta N_{\text{sub}} \left(\frac{\partial \bar{N}_{\text{sub}}}{\partial \phi}\right)^{-1} = \sqrt{2}\Delta N \left(2\frac{\partial \bar{N}}{\partial \phi}\right)^{-1}$$
$$= \frac{1}{\sqrt{2}}\Delta N \left(\frac{\partial \bar{N}}{\partial \phi}\right)^{-1} = \frac{\delta\phi}{\sqrt{2}}. \tag{7}$$

However, in our implementation we use a random realization of photon subtraction. The random nature of the postselection loss leads to removing events from the analysis. These events may contain information about the measurement, and removing them reduces the sensitivity.

As mentioned, to take the number of measurements into account, $s = m\bar{N}$. Similarly, the standard deviation expression picks up a factor of $\sqrt{m}$. The implication is that $\delta\phi$ decreases by a factor of $1/\sqrt{m}$ as the number of measurements increases. Let us assume that ξ percent of measurements leads to subtraction. In that case, $\delta\phi_{\text{sub}}$ scales with $1/\sqrt{2\xi m}$ as a function of the total number of measurements. One can show that in this case

$$\delta\phi_{\text{sub}} = \frac{\delta\phi}{\sqrt{2\xi}}. \tag{8}$$

Thus for a random subtraction procedure to be practical one has to reduce the subtraction loss to at least 50%. Recently, there has been progress in realizing a highly efficient scheme for subtracting exactly one photon from an optical beam [27]. Although sub-

tracting exactly one photon is not entirely equivalent to "photon subtraction" (as noted by the authors in [27]), their result suggests that the realization of photon-subtraction schemes with high efficiency could be a possibility. Given this exciting prospect, our experiment constitutes an important first step in developing useful applications of photon-subtracted states in interferometry.

5. SUMMARY

In summary, we have proposed and realized a procedure based on photon subtraction for increasing the SNR with which one can measure the phase shift induced on a thermal light field with occupation number of fewer than four photons. We have implemented this method for a single-transverse-mode thermal light field. This procedure could be generalized to increase the measurement sensitivity for each spatial mode of a multimode light field, a procedure that holds great promise for increasing the sensitivity of image formation of objects illuminated only by weak thermal light fields.

Interferometry is inherently related to imaging, as demonstrated by the Michelson stellar interferometer/van Cittert Zernike theorem. As such, an enhanced method of interferometry for thermal light can potentially benefit all imaging applications that rely on thermal sources of radiation.

Funding. Defense Advanced Research Projects Agency (DARPA).

Acknowledgment. We acknowledge funding from the Defense Advanced Research Projects Agency.

See Supplement 1 for supporting content.

REFERENCES AND NOTES

1. B. P. Abbott, et al., "Observation of gravitational waves from a binary black hole merger," Phys. Rev. Lett. **116**, 061102 (2016).
2. C. M. Caves, "Quantum limits on noise in linear-amplifiers," Phys. Rev. D **26**, 1817–1839 (1982).
3. C. M. Caves, "Quantum-mechanical noise in an interferometer," Phys. Rev. D **23**, 1693–1708 (1981).
4. P. Grangier, R. E. Slusher, B. Yurke, and A. LaPorta, "Squeezed-light-enhanced polarization interferometer," Phys. Rev. Lett. **59**, 2153–2156 (1987).
5. V. Giovannetti, S. Lloyd, and L. Maccone, "Quantum-enhanced measurements: beating the standard quantum limit," Science **306**, 1330–1336 (2004).
6. V. Giovannetti, S. Lloyd, and L. Maccone, "Quantum metrology," Phys. Rev. Lett. **96**, 010401 (2006).
7. C. C. Gerry and J. Mimih, "The parity operator in quantum optical metrology," Contemp. Phys. **51**, 497–511 (2010).
8. V. Giovannetti, S. Lloyd, and L. Maccone, "Advances in quantum metrology," Nat. Photonics **5**, 222–229 (2011).
9. M. D'Angelo, M. V. Chekhova, and Y. Shih, "Two-photon diffraction and quantum lithography," Phys. Rev. Lett. **87**, 013602 (2001).
10. R. A. Campos, C. C. Gerry, and A. Benmoussa, "Optical interferometry at the Heisenberg limit with twin Fock states and parity measurements," Phys. Rev. A **68**, 023810 (2003).
11. M. W. Mitchell, J. S. Lundeen, and A. M. Steinberg, "Super-resolving phase measurements with a multiphoton entangled state," Nature **429**, 161–164 (2004).
12. P. Walther, J. W. Pan, M. Aspelmeyer, R. Ursin, S. Gasparoni, and A. Zeilinger, "De Broglie wavelength of a non-local four-photon state," Nature **429**, 158–161 (2004).
13. T. Nagata, R. Okamoto, J. L. O'Brien, K. Sasaki, and S. Takeuchi, "Beating the standard quantum limit with four-entangled photons," Science **316**, 726–729 (2007).
14. M. Kacprowicz, R. Demkowicz-Dobrzański, W. Wasilewski, K. Banaszek, and I. A. Walmsley, "Experimental quantum-enhanced estimation of a lossy phase shift," Nat. Photonics **4**, 357–360 (2010).
15. M. A. Usuga, C. R. Müller, C. Wittmann, P. Marek, R. Filip, C. Marquardt, G. Leuchs, and U. L. Andersen, "Noise-powered probabilistic concentration of phase information," Nat. Phys. **6**, 767–771 (2010).
16. F. Ferreyrol, M. Barbieri, R. Blandino, S. Fossier, R. Tualle-Brouri, and P. Grangier, "Implementation of a nondeterministic optical noiseless amplifier," Phys. Rev. Lett. **104**, 123603 (2010).
17. G. Y. Xiang, T. C. Ralph, A. P. Lund, N. Walk, and G. J. Pryde, "Heralded noiseless linear amplification and distillation of entanglement," Nat. Photonics **4**, 316–319 (2010).
18. A. Zavatta, J. Fiurášek, and M. Bellini, "A high-fidelity noiseless amplifier for quantum light states," Nat. Photonics **5**, 52–60 (2011).
19. J. Park, J. Joo, A. Zavatta, M. Bellini, and H. Jeong, "Efficient noiseless linear amplification for light fields with larger amplitudes," Opt. Express **24**, 1331–1346 (2016).
20. V. Parigi, A. Zavatta, M. Kim, and M. Bellini, "Probing quantum commutation rules by addition and subtraction of single photons to/from a light field," Science **317**, 1890–1893 (2007).
21. Y. Zhai, F. E. Becerra, B. L. Glebov, J. Wen, A. E. Lita, B. Calkins, T. Gerrits, J. Fan, S. W. Nam, and A. Migdall, "Photon-number-resolved detection of photon-subtracted thermal light," Opt. Lett. **38**, 2171–2173 (2013).
22. J. Wenger, R. Tualle-Brouri, and P. Grangier, "Non-Gaussian statistics from individual pulses of squeezed light," Phys. Rev. Lett. **92**, 153601 (2004).
23. A. Ourjoumtsev, R. Tualle-Brouri, J. Laurat, and P. Grangier, "Generating optical Schrödinger kittens for quantum information processing," Science **312**, 83–86 (2006).
24. J. S. Neergaard-Nielsen, B. M. Nielsen, C. Hettich, K. Mølmer, and E. S. Polzik, "Generation of a superposition of odd photon number states for quantum information networks," Phys. Rev. Lett. **97**, 083604 (2006).
25. A. Ourjoumtsev, F. Ferreyrol, R. Tualle-Brouri, and P. Grangier, "Preparation of non-local superpositions of quasi-classical light states," Nat. Phys. **5**, 189–192 (2009).
26. H. Takahashi, J. S. Neergaard-Nielsen, M. Takeuchi, M. Takeoka, K. Hayasaka, A. Furusawa, and M. Sasaki, "Entanglement distillation from Gaussian input states," Nat. Photonics **4**, 178–181 (2010).
27. S. Rosenblum, O. Bechler, I. Shomroni, Y. Lovsky, G. Guendelman, and B. Dayan, "Extraction of a single photon from an optical pulse," Nat. Photonics **10**, 19–22 (2016).
28. R. Carranza and C. C. Gerry, "Photon-subtracted two-mode squeezed vacuum states and applications to quantum optical interferometry," J. Opt. Soc. Am. B **29**, 2581–2587 (2012).
29. R. Birrittella and C. C. Gerry, "Quantum optical interferometry via the mixing of coherent and photon-subtracted squeezed vacuum states of light," J. Opt. Soc. Am. B **31**, 586–588 (2014).
30. D. Braun, P. Jian, O. Pinel, and N. Treps, "Precision measurements with photon-subtracted or photon-added Gaussian states," Phys. Rev. A **90**, 013821 (2014).
31. M. D. Vidrighin, O. Dahlsten, M. Barbieri, M. S. Kim, V. Vedral, and I. A. Walmsley, "Photonic Maxwell's demon," Phys. Rev. Lett. **116**, 050401 (2016).
32. e.g., Eq. (2) can be derived using a procedure described in Chap. 6 of C. C. Gerry and P. Knight, *Introductory Quantum Optics* (Cambridge University, 2004).
33. A. Zavatta, V. Parigi, M. S. Kim, H. Jeong, and M. Bellini, "Experimental demonstration of the bosonic commutation relation via superpositions of quantum operations on thermal light fields," Phys. Rev. Lett. **103**, 140406 (2009).
34. C. G. Parazzoli, B. E. Koltenbah, D. R. Gerwe, P. S. Idell, B. T. Gard, R. Birrittella, S. M. Hashemi Rafsanjani, M. Mirhosseini, O. S. Magana-Loaiza, J. P. Dowling, C. C. Gerry, R. W. Boyd, and B. C. Capron, "Enhanced thermal object imaging by photon addition and subtraction," arXiv:1609:02780 (2016).
35. F. T. Arecchi, "Measurement of the statistical distribution of Gaussian and laser sources," Phys. Rev. Lett. **15**, 912–916 (1965).
36. J. Honer, R. Löw, H. Weimer, T. Pfau, and H. P. Büchler, "Artificial atoms can do more than atoms: deterministic single photon subtraction from arbitrary light fields," Phys. Rev. Lett. **107**, 093601 (2011).
37. C. I. Osorio, N. Bruno, N. Sangouard, H. Zbinden, N. Gisin, and R. T. Thew, "Heralded photon amplification for quantum communication," Phys. Rev. A **86**, 023815 (2012).

optica

Quantum-enhanced interferometry with weak thermal light: supplementary material

SEYED MOHAMMAD HASHEMI RAFSANJANI[1,*], MOHAMMAD MIRHOSSEINI[1], OMAR S. MAGAÑA-LOAIZA[1], BRYAN T. GARD[2], RICHARD BIRRITTELLA[3], B. E. KOLTENBAH[4], C. G. PARAZZOLI[4], BARBARA A. CAPRON[4], CHRISTOPHER C. GERRY[3], JONATHAN P. DOWLING[2], AND ROBERT W. BOYD[1,5]

[1] *Institute of Optics, University of Rochester, Rochester, New York 14627*
[2] *Hearne Institute for Theoretical Physics and Department of Physics and Astronomy, Louisiana State University, Baton Rouge, LA 70803*
[3] *Department of Physics and Astronomy, Lehman College, The City University of New York, Bronx, New York 10468*
[4] *Boeing Research & Technology, Seattle, WA 98124*
[5] *Department of Physics, University of Ottawa, Ottawa, ON, K1N6N5, Canada*
[*] *Corresponding author: shashem2@ur.rochester.edu*

Published 20 April 2017

This document provides supplementary information to "Quantum-enhanced interferometry with weak thermal light," https://doi.org/10.1364/optica.4.000487. The mathematical model behind photon subtraction, a discussion on the photon distribution, an explanation about common-path interferometers, and information on the photon counting scheme are presented below.

https://doi.org/10.1364/optica.4.000487.s001

1. PHOTON SUBTRACTION

In the following we present a detailed calculation of the effect of the subtraction on the quantum state of a photon that leaves a Mach-Zehnder interferometer. The two input ports of the interferometer (a, b) are fed by a thermal state and the vacuum state respectively (See Fig. S1). Let us first derive the the reduced density matrix at the two output ports (c, d). A schematic version of the model is given in Fig. S1 The output ports are related to the input ports through a unitary transformation:

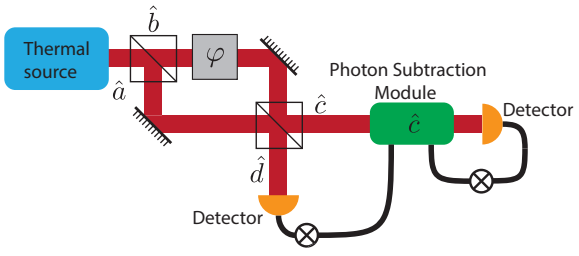

Fig. S1. Conceptual representation of a thermal interferometry experiment to observe the enhancement of signal and signal-to-noise ratio as result of photon subtraction.

$$\hat{c} = \frac{1}{2}\left\{iy\hat{a} - x\hat{b}\right\}$$
$$\hat{d} = \frac{1}{2}\left\{iy\hat{b} + x\hat{a}\right\} \quad \textbf{(S1)}$$

where $x = 1 - e^{i\varphi}$, and $y = e^{i\varphi} + 1$. The input state is given by

$$\hat{\rho}_0 = \sum_n \frac{\bar{n}^n}{(1+\bar{n})^{n+1}} |n\rangle_a \, {}_a\langle n| \otimes |0\rangle_b \, {}_b\langle 0|. \quad \textbf{(S2)}$$

The reduced density matrix of the state at port c can be derived by taking a partial trace on d:

$$\hat{\rho}_{0c} = \mathrm{Tr}_d[\hat{\rho}_0] = \sum_{m=0}^{\infty} {}_d\langle m|\hat{\rho}_0|m\rangle_d \quad \textbf{(S3)}$$

To evaluate this density matrix we need to calculate the following quantity

$$\begin{aligned}\mathcal{A}_{m,n} &= {}_d\langle m| \otimes {}_c\langle n|\hat{\rho}_0|n\rangle_c \otimes |m\rangle_d \\ &= \frac{1}{m!n!} {}_d\langle 0| \otimes {}_c\langle 0|d^m c^n \hat{\rho}_0 c^{\dagger n} d^{\dagger m}|0\rangle_c \otimes |0\rangle_d \end{aligned} \quad \textbf{(S4)}$$

Note that $|0\rangle_c \otimes |0\rangle_d = |0\rangle_a \otimes |0\rangle_b$, and we can expand this expression to evaluate it;

$$\begin{aligned}\mathcal{A}_{m,n} &= \frac{1}{m!n!4^{m+n}}\, {}_a\langle 0| \otimes {}_b\langle 0|(-x\hat{b}+iy\hat{a})^n \\ &\quad (iy\hat{b}+x\hat{a})^m \hat{\rho}_{th}^{(a)} \otimes |0\rangle_b\, {}_b\langle 0|(-iy\hat{b}^\dagger + x\hat{a}^\dagger)^m \\ &\quad (-x\hat{b}^\dagger - iy\hat{a}^\dagger)^n |0\rangle_a \otimes |0\rangle_b \\ &= \frac{|x|^{2m}|y|^{2n}}{m!n!4^{m+n}}\, {}_a\langle 0|\hat{a}^{n+m}\hat{\rho}_{th}^{(a)}\hat{a}^{\dagger(n+m)}|0\rangle_a \\ &= \frac{|x|^{2m}|y|^{2n}}{m!n!4^{m+n}} \sum_i \frac{\bar{n}^i |\,{}_a\langle 0|\hat{a}^{n+m}|i\rangle_a|^2}{(1+\bar{n})^{i+1}} \\ &= \frac{|x|^{2m}|y|^{2n}(m+n)!}{m!n!4^{m+n}} \frac{\bar{n}^{m+n}}{(1+\bar{n})^{m+n+1}} \end{aligned} \quad \textbf{(S5)}$$

Using this result one can calculate the diagonal elements of the reduced density matrix.

$$\begin{aligned}{}_c\langle n|\hat{\rho}_c|n\rangle_c &= \sum_m \mathcal{A}_{m,n} \\ &= \frac{|y|^{2n}\bar{n}^n}{4^n(1+\bar{n})^{n+1}} \sum_m \binom{n+m}{m} \left(\frac{\bar{n}|x|^2}{4(1+\bar{n})}\right)^m \\ &= \frac{|y|^{2n}\bar{n}^n}{4^n(1+\bar{n})^{1+n}} \left(\frac{1}{1-\frac{\bar{n}|x|^2}{4(1+\bar{n})}}\right)^{n+1} \\ &= \frac{|y|^{2n}\bar{n}^n}{4^n} \frac{1}{(1+\frac{\bar{n}|y|^2}{4})^{n+1}} \end{aligned} \quad \textbf{(S6)}$$

Furthermore one can readily confirm that $\langle i|\hat{\rho}_c|j\rangle$ vanishes if $i \neq j$. Thus the density matrix at port $\hat{c}$ can be written as

$$\hat{\rho}_c = \sum_n \frac{(\bar{n}\cos^2\frac{\varphi}{2})^n}{(1+\bar{n}\cos^2\frac{\varphi}{2})^{n+1}} |n\rangle_c\, {}_c\langle n| \quad \textbf{(S7)}$$

which a thermal state with the reduced occupation number and standard deviation of

$$\bar{n}_c = \mathrm{Tr}[\hat{c}^\dagger\hat{c}\hat{\rho}_c] = \bar{n}\cos^2\frac{\varphi}{2}, \qquad \sigma_c = \sqrt{\bar{n}_c^2 + \bar{n}_c} \quad \textbf{(S8)}$$

Similarly one can show that the reduced density matrix at port $\hat{d}$ is a thermal state with the reduced occupation number and standard deviation of

$$\bar{n}_d = \mathrm{Tr}[\hat{d}^\dagger\hat{d}\hat{\rho}_0] = \bar{n}\sin^2\frac{\varphi}{2}, \qquad \sigma_d = \sqrt{\bar{n}_d^2 + \bar{n}_d} \quad \textbf{(S9)}$$

Next we study the effect of photon subtraction on the reduced density matrices at output ports. Subtracting a photon in port $\hat{c}$ can be described by the following operation:

$$\hat{\rho}_0 \to \hat{\rho}_1 = \frac{\hat{c}\hat{\rho}_0\hat{c}^\dagger}{\mathrm{Tr}[\hat{c}\hat{\rho}_0\hat{c}^\dagger]}. \quad \textbf{(S10)}$$

By taking partial trace one can then find the reduced density matrix at each of the output ports.

$$\hat{\rho}_{1c} = \mathrm{Tr}_d[\hat{\rho}_1].$$

First we note that

$${}_d\langle m| \otimes {}_c\langle n|\hat{\rho}_1|n\rangle_c \otimes |m\rangle_d = \frac{n+1}{\bar{n}_c}\mathcal{A}_{m,n+1} \quad \textbf{(S11)}$$

Thus the diagonal elements of the reduced density matrix can be found as following

$${}_c\langle n|\hat{\rho}_c|n\rangle_c = \frac{n+1}{\bar{n}_c}\sum_m \mathcal{A}_{m,n+1} = \frac{(n+1)\bar{n}_c^n}{(1+\bar{n}_c)^{n+2}} \quad \textbf{(S12)}$$

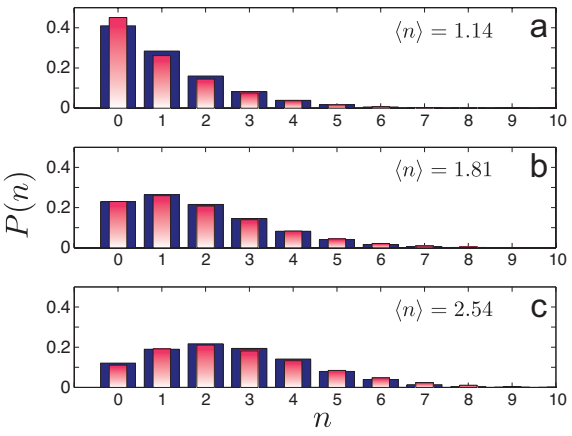

Fig. S2. (a) Photon distribution for the thermal light distribution that we used in the experiment. (b) Photon number distribution for the photon-subtracted thermal light. (c) Photon number distribution for the two-photon-subtracted thermal light. The dark bars represent the experimental results and the bright bars are the corresponding theory predictions.

One can readily confirm that the off-diagonal elements are all zero and thus the reduced density matrix in port $\hat{c}$ after the subtraction are given by

$$\hat{\rho}_{1c} = \sum_n \frac{(n+1)\bar{n}_c^n}{(1+\bar{n}_c)^{n+2}} |n\rangle_c\, {}_c\langle n|. \quad \textbf{(S13)}$$

The average occupation number and the standard deviation of this distribution are

$$\begin{aligned}\mathrm{Tr}[\hat{c}^\dagger\hat{c}\hat{\rho}_1] &= 2\bar{n}\cos^2\frac{\varphi}{2} = 2\bar{n}_c \\ (\mathrm{Tr}[(\hat{c}^\dagger\hat{c})^2\hat{\rho}_1] - \mathrm{Tr}[\hat{c}^\dagger\hat{c}\hat{\rho}_1]^2)^{1/2} &= \sqrt{2}\sigma_c \end{aligned} \quad \textbf{(S14)}$$

Note that the standard deviation increases only by a factor of $\sqrt{2}$ whereas the signal is multiplied by a factor of 2, and thus the signal-to-noise ratio is enhanced by a factor of $\sqrt{2}$. Similarly one can show that the conditioned on subtracted events in mode $\hat{c}$ the average occupation number in port $\hat{d}$ doubles and the standard deviation is enhanced by a factor of $\sqrt{2}$ too.

$$\begin{aligned}\mathrm{Tr}[\hat{d}^\dagger\hat{d}\hat{\rho}_1] &= 2\bar{n}\sin^2\frac{\varphi}{2} = 2\bar{n}_d \\ (\mathrm{Tr}[(\hat{d}^\dagger\hat{d})^2\hat{\rho}_1] - \mathrm{Tr}[\hat{d}^\dagger\hat{d}\hat{\rho}_1]^2)^{1/2} &= \sqrt{2}\sigma_d \end{aligned} \quad \textbf{(S15)}$$

We emphasize that this surprising result could be expected since, in contrast with the input ports, the density matrix at the output ports are correlated.

2. PHOTON DISTRIBUTION

When a beam of light that can be described by a coherent state is passed through a rotating ground glass light is scattered in a speckle pattern. If light from this scattering is coupled into a single-mode fiber the emerging light possess thermal distribution. In Fig. (S2 a) we plot this distribution and compare it with the theory. For the sake of completeness we have also included plots for the one-photon subtracted state and two-photon subtracted states in Fig. (S2 b) and Fig. (S2 c)

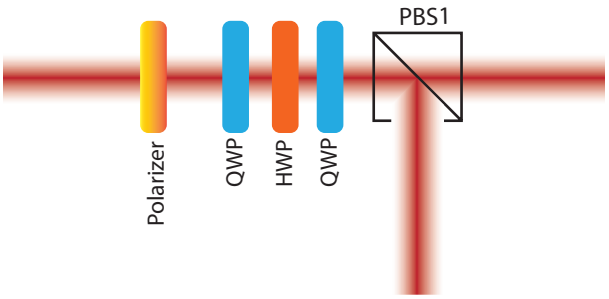

Fig. S3. A schematic representation of a common-path Mach-Zehnder interferometer that induces a variable phase between the two polarizations.

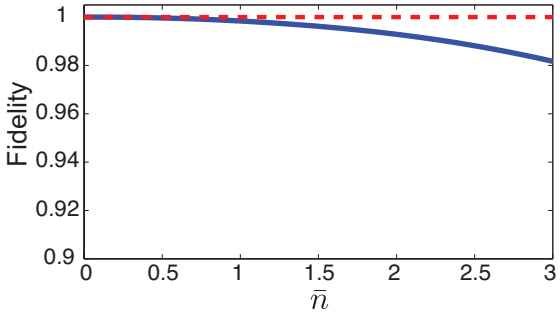

Fig. S4. The fidelity between the probability distribution of thermal statistics and the probability distribution detected by our photon counting scheme for thermal lights of different values of average occupation number.

3. COMMON PATH MACH-ZEHNDER INTERFEROMETER

In a conventional Mach-Zehnder interferometer the first beam splitter separates the beam into two parts. Each part takes a separate path and and then we bring the two paths together and recombine them using another beam splitter. The difference between the accumulated phase of the paths determines the intensity distribution at the two output ports. A challenging aspect of an MZI is its stability; A slight instability in any of the components would lead to phase instability and diminishes the fringe visibility. To alleviate this problem one can replace the two spatially separated paths by polarization, and uses wave plates to induce a phase between the two polarizations. As such one no longer needs to separate the two polarizations spatially, and can considerably mitigate the instability of the system.

Below we present a detailed discussion on how this interferometer works. In Fig. S3 we present a schematic representation of a common-path Mach-Zehnder interferometer. The polarizer prepares the polarization state $|H\rangle$ which can be written as an equally wighted coherent superposition of $|D\rangle$ and $|A\rangle$. Note that here

$$|D\rangle = \frac{|H\rangle + |V\rangle}{\sqrt{2}},$$
$$|A\rangle = \frac{|H\rangle - |V\rangle}{\sqrt{2}}. \quad \textbf{(S16)}$$

Our aim is to induce a phase between the two components $|D\rangle$ and $|A\rangle$. Then we set a quarter wave-plate (QWP) in a 45° angle. The QWP maps $|D\rangle \rightarrow |R\rangle$, and $|A\rangle \rightarrow |L\rangle$ where

$$|R\rangle = \frac{|H\rangle + i|V\rangle}{\sqrt{2}},$$
$$|L\rangle = \frac{|H\rangle - i|V\rangle}{\sqrt{2}}. \quad \textbf{(S17)}$$

Next we can use a half wave-plate that induces a variable phase between the two components $|R\rangle$ and $|L\rangle$. Again a QWP can be used to map $|R\rangle \rightarrow |D\rangle$ and $|L\rangle \rightarrow |A\rangle$, and finally we use a polarizing beam splitter to separate the two polarizations $|D\rangle$ and $|A\rangle$. By rotating the HWP we can change the induced phase between the two polarizations $|D\rangle$ and $|A\rangle$ and we get a one-to-one mapping between this setup and a conventional Mach-Zehnder interferometer.

4. SURJECTIVE PHOTON COUNTING

We emphasize that the effect of the inherent quantum efficiency of the detector can be modeled by combination of a beam splitter and a detector of quantum efficiency of 100%. That is a detector that fires if at least one photon arrives. Thus for simplifying our analysis we assume a detector with detection efficiency of 100%. For thermal light with average occupation number of $\bar{n}$ the probability of incurring an N-photon event is given by

$$P(N) = \frac{\bar{n}^N}{(1+\bar{n})^{N+1}}. \quad \textbf{(S18)}$$

In our surjective detection scheme this event may be registered as a detection of a lower number of photons if more than one photons arrive separated by less than the dead time of the detector. Assuming that the dead time of the detector time is $\sim 50\,ns$ and the coherence time of the source is $\sim\ 1\mu s$ in each coherence time there are $K = 20$ time bins. In principle an N-photon event can be registered as any of $\{1, 2, \cdots, N\}$-photon events, and since we work with very few photons we assume that always $K > N$. Then the probability distribution of number of clicks if N photons arrive in a temporal mode can be cast as a combinatorics problem and one uses Bayes' theorem:

$$P(m) = \sum_N P(N)P(m|N). \quad \textbf{(S19)}$$

to find the modified probability distribution, $P(m)$, that the APDs register. In Fig. S4 we plot the fidelity between the probability distribution of the thermal statistics and the probability distribution detected by the our surjective counting scheme. Fidelity is a measure of distance between any two probability distributions. The fidelity of two probability distributions $\{q_i\}$ and $\{p_i\}$ is defined by $\sum_i \sqrt{p_i q_i}$ and its range between $\{0, 1\}$ [1]. The high value of the fidelity confirms our initial intuition that for low photon number, our counting scheme provides an excellent approximation to the actual photon distribution. Finally it should be noted that to compare with the experimental results one can feed the probability distributions that are predicted by the theory into an algorithm that counts for the surjective nature of the counting mechanism before comparing them to the experimental results.

REFERENCES

1. M. A. Nielsen and I. L. Chuang, *Quantum Computation and Quantum Information*, 10th Anniversary Edition (Cambridge University Press, Cambridge, 2009).